

CORONARY ANGIOGRAPHY

Dynamic Real-Time Architecture in Magnetic Resonance Coronary Angiography—A Prospective Clinical Trial

Phillip C. Yang, M.D.,^{1,*} Juan M. Santos, M.S.,²
Patricia K. Nguyen, M.D.,¹ Greig C. Scott, Ph.D.,² Jan Engvall, M.D.,¹
Michael V. McConnell, M.D., M.S.E.E.,¹ Graham A. Wright, Ph.D.,³
Dwight G. Nishimura, Ph.D.,³ John M. Pauly, Ph.D.,²
and Bob S. Hu, M.D.²

¹Division of Cardiovascular Medicine, Department of Medicine, Stanford University Medical Center, Stanford, California, USA

²Magnetic Resonance Systems Research Laboratory, Department of Electrical Engineering, Stanford University, Stanford, California, USA

³General Electric Medical Systems, Menlo Park, California, USA

ABSTRACT

Objectives: A dynamic real-time (*dRT*) architecture has been developed to address limitations in magnetic resonance coronary angiography (MRCA). A prospective clinical trial of 45 patients suspected of coronary artery disease was conducted to determine clinical utility of this integrated real-time system. *Background:* Clinical implementation of MRCA is not performed routinely today. However, improved anatomic coverage, image quality, and scan flexibility may enhance its clinical utility. A novel real-time architecture addresses these challenges through instantaneous reconfiguration between real-time (RT) and high-resolution (HR) imaging sequences with dynamic selection of the desired element on a custom-designed receiver coil. *Methods:* A total of 45 subjects were recruited consecutively to evaluate scan time, anatomic coverage, image quality, and detection of coronary lesions. Using a modern PC, the *dRT* switches from RT to gated HR imaging sequence in one repetition time (39 ms). Magnetic resonance imaging (MRI) scanning was performed using a custom-designed coronary coil consisting of two four-inch phase-array circular elements enabled with real-time selection of the desired coil element. *Results:* All studies were completed in less than 45 minutes and required a mean of 12 breath holds (16 heartbeats). Of the total number of coronary segments, 91% (357/394) were

*Correspondence: Phillip C. Yang, M.D., Division of Cardiovascular Medicine, Department of Medicine, Stanford University Medical Center, 300 Pasteur Drive, Room H-2157, Stanford, CA 94305-5233, USA; Fax: (650) 724-4034; E-mail: pyang@cvmed.stanford.edu.

visualized. Excellent or good image quality was achieved in 86% of the segments. Blinded analysis of the coronary arteries revealed sensitivity of 93% and specificity of 88% in the detection of coronary stenoses. *Conclusions:* The integrated environment of *dRT* provides a rapid and flexible scan protocol for MRCA while achieving wide anatomical coverage, high image quality, and reliable detection of coronary stenosis in short scan time.

Key Words: Magnetic resonance coronary angiography; Dynamic real-time imaging; Coronary artery disease.

INTRODUCTION

Routine clinical implementation of magnetic resonance coronary angiography (MRCA) continues to face limitations. The coronary arteries are small, tortuous, embedded in tissue with competing magnetic resonance (MR) signals, and move asynchronously due to cardiac and respiratory motions. Suboptimal image quality, inadequate anatomic coverage, and tedious scan protocols are well-known challenges in MRCA. Recent clinical studies have reported improved MRCA images (Kim et al., 2001; Li et al., 2001; Yang et al., 2003a). However, improvement in signal, anatomic coverage, and scan flexibility will further enhance the clinical utility of this technique. In order to address these issues, a dynamic real-time architecture (*dRT*) with novel properties has been developed.

The *dRT* has been designed to improve essential features in MRCA. First, dynamic reconfiguration between real-time (RT) and high-resolution (HR) pulse sequences enhances scan flexibility. A rapid RT localization of the coronary artery followed by an instantaneous switch to HR imaging in one repetition time (TR) allows image-based feedback to assess image quality and anatomic coverage. If the segment is poorly imaged due to a suboptimal scan plane or if further characterization is necessary, a rapid RT adjustment of the plane followed by HR reacquisition of the coronary segment is possible. Incorporated into the *dRT* architecture is a dedicated coronary coil that is designed to enhance signal-to-noise ratio (SNR) and anatomic coverage. The coil consists of two 4-inch phased-array circular receiver elements overlapped in a linear array. The *dRT* enables instantaneous selection of the coil element to target distal segments without compromising SNR.

This integrated system designed to enhance scan flexibility, coverage, and SNR underwent a prospective trial to determine its clinical utility. Forty-five patients suspected of coronary artery disease (CAD) were studied consecutively. Systematic analysis of the scan

duration, anatomic coverage, image quality, and detection of coronary stenoses was performed.

METHODS

Patient Population

A total of 45 patients (33 males, 12 females; aged 40 to 86 years; weight 70 to 120 kg) referred for X-ray coronary angiography was enrolled sequentially in the study. Baseline patient and coronary characteristics are listed in Table 1. All 45 patients underwent MRCA within one month before X-ray coronary angiography. The study protocol was approved by the Human Subjects Committee at Stanford University. The patients were enrolled from both Stanford and Palo Alto Veterans Administration Medical Centers. All participants were informed of the study and gave written

Table 1. Baseline patient characteristics.

Patient characteristics	
Mean age (range)	62 (40–80)
Male (%)	35 (78%)
Mean weight kg (range)	84 (60–120)
Prior myocardial infarction (%)	15 (33%)
CAD (%)	23 (51%)
Stent placement (%)	11 (24%)
CAD location (per vessel)	
LM	2
LAD	16
LCx	10
RCA	12
CAD extent (per patient)	
Single vessel	13
Two vessel	5
Multi-vessel (≥ 3)	5

Abbreviations: RCA=right coronary artery; LM=left main artery; LAD=left anterior descending artery; LCx=left circumflex artery; and CAD=coronary artery disease.

informed consent. Patients were ineligible if they had arrhythmias, unstable clinical condition, coronary artery bypass graft surgery, or contraindications to undergo MRI scan as listed on the screening form.

Protocol

Study patients underwent *d*RT imaging in the supine position. The protocol consisted of RT localization without breath holding or cardiac gating followed immediately by end-expiratory breath-held and cardiac-gated HR imaging. When further optimization of HR image quality was necessary, the protocol was repeated. The *d*RT architecture enabled instantaneous switching between RT and HR sequences facilitating such an optimization process. The HR triggered to the cardiac cycle using a plethysmogram and required breath-holding duration of 16 heartbeats. Three slices, each 5-mm thick with 20% overlap, were obtained with each breath hold. A customized coronary surface coil was used for signal reception as described below.

MR Scanner

A 1.5T GE Signa LX MRI Scanner (GE, Milwaukee, WI) equipped with high-performance gradients capable of 40 mT/m amplitude and 150 mT/m/ms slew rate was used.

Dynamic Real-Time Architecture (*d*RT)

A detailed description of *d*RT has been reported by Santos et al. (2002). Briefly, the *d*RT enables reconfiguration of a pulse sequence within a scan repetition time (TR). A modern PC (AMD, Santa Clara, CA) schedules the imaging sequence and calculates the waveform to generate a scan protocol and pulse sequence on the fly. This capability implemented in a real-time imaging environment enables interactive selection of a desired imaging sequence due to simultaneous sharing of data and resources among different sequences. This architecture, based on the concept of the virtual machine in computer science, enables the implementation of a real-time virtual scanner. A virtual scanner enables sharing of limited resources such as hardware and magnetization between different sequences so that each sequence may utilize the available resources for its own purposes. The *d*RT architecture consists of two main components: master scheduler and sequence generator. A master scheduler selects the pulse sequence, acquisition, reconstruction, and display modes necessary in a particular imaging mode. A sequence generator then calculates the waveform and timing parameters necessary to run the pulse sequence. Once the sequence has been played out, the data are reconstructed and displayed according to the needs of the specific pulse sequence. In this environment, the

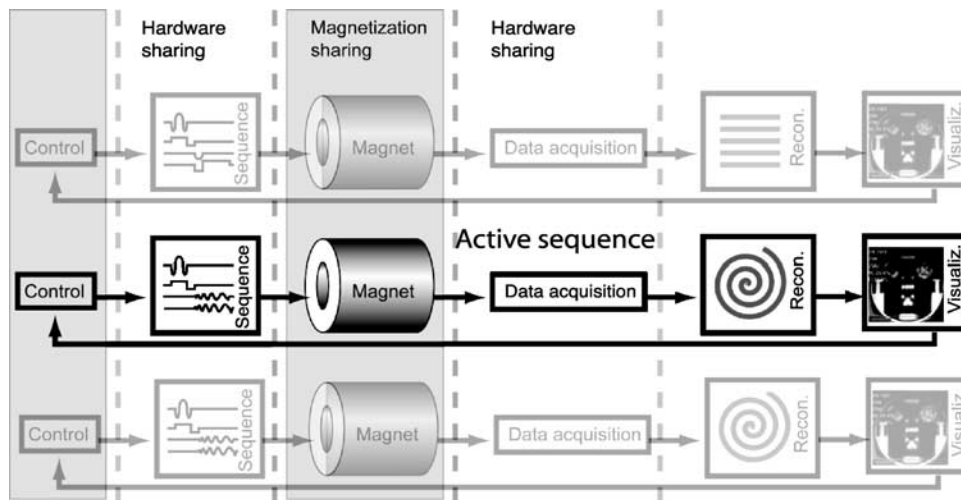


Figure 1. A schematic diagram of the virtual scanner demonstrating the concept of rapid switching among multiple imaging sequences through sharing of hardware and magnetization. Any protocol is selected on-the-fly and is enabled to utilize the entire resource available.

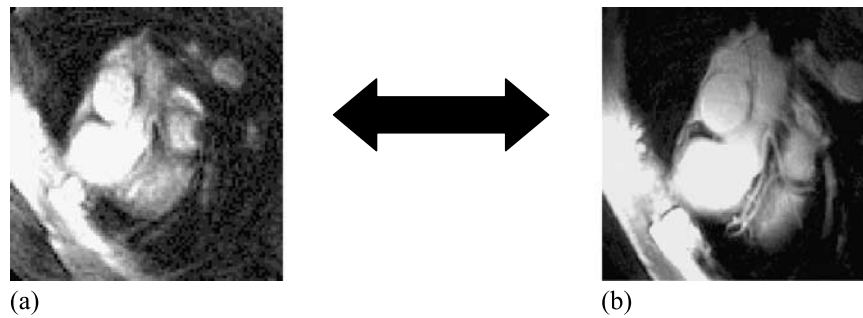


Figure 2. Rapid switch between (a) RT localization and (b) HR image of LAD and LCx is possible.

resources are shared but each sequence proceeds as if all the resources are made available to it (Fig. 1).

The dRT images the coronary arteries through a rapid switch (39 ms) between RT localization and two-dimensional (2D) multi-slice HR imaging as shown in Fig. 2 (Kerr et al., 1997; Meyer et al., 1992; Yang et al., 2003a). The RT and HR sequences share the same spectral-spatial pulse for fat suppression and water excitation (11-ms) and spiral read-out gradient (16 ms and 4096 data points per interleaf) generating identical repetition time (TR) (39 ms), echo time (4.9 ms), and field of view (FOV) (20 cm). The different variables are the number of spiral interleaves, flip angle, and the resultant spatial and temporal resolution. The RT utilizes three interleaves and 30° flip angle to generate 1.9-mm spatial resolution and nine frames/sec using

sliding window reconstruction. The HR implements 16 interleaves and 60° flip angle to achieve spatial resolution of 0.72 mm and temporal resolution of 39-ms/slice with acquisition occurring in diastole (330-ms trigger-delay).

Customized Coronary Coil

A prototype two-element phased-array coronary receiver coil was constructed to achieve higher SNR and anatomical coverage (Engvall et al., 2003). The two circular coil elements each designed with a smaller diameter of 4-in. provide higher SNR than standard 5-in. surface coil or phased array cardiac coil (6-in. coil element). In order to achieve higher FOV, there are two coil elements. They are overlapped in a linear

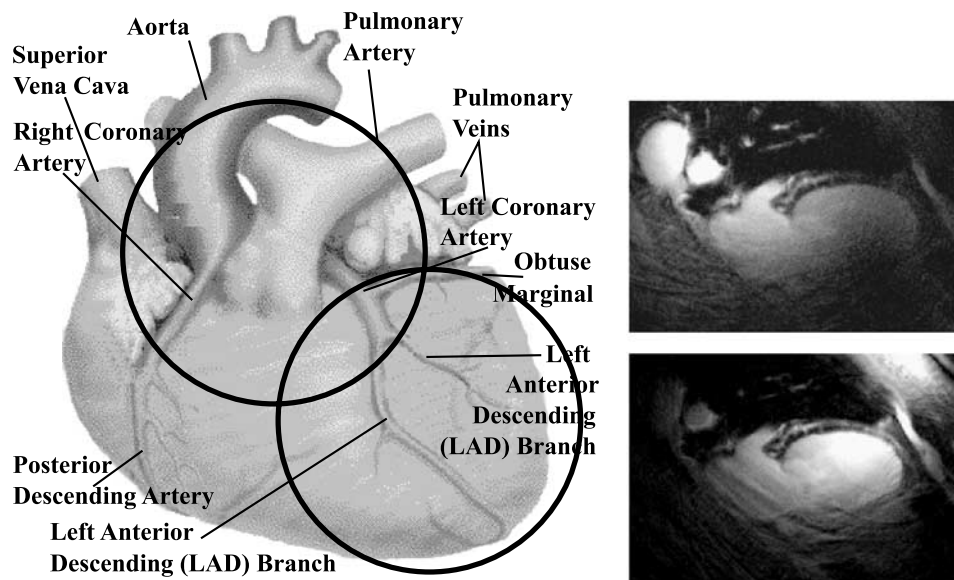


Figure 3. A schematic diagram of the dedicated coronary coil demonstrating coverage of the two overlapping 4-in. coil elements. The proximal coil targets proximal LAD and the distal coil targets the distal LAD.

array to eliminate mutual inductance. Each coil is split into four quadrants with distributed capacitors to minimize dielectric loss. A combination of passive and PIN diode blocking is placed to reduce any interaction with the RF transmitter pulses. Finally, in order to reduce cable interactions due to unbalanced currents on the outer layer of coaxial cable, current mode baluns are built to function as cable traps. This two-element phased-array coil is placed in cranial-caudal position along the subject's left chest. This flexible design allows targeted imaging of the coronary anatomy while maintaining a sensitivity volume higher than a standard 5-in. surface coil. In addition, the larger coverage of the dedicated coil allowed ease of coil placement relative to the position of patient's heart. The proximal coil targets the proximal and mid-right coronary artery (RCA), proximal-left circumflex artery (LCx), left main, and proximal-left anterior descending (LAD). The distal coil targets the mid-and distal LAD, distal-RCA, and distal-LCx. The *d*RT enables switching between the two coils in real time and reconstruct HR images from individual or both coils. A schematic diagram of the coronary coil and its coverage of proximal and distal LAD are shown in Fig. 3.

Data Evaluation

All MRCA images were evaluated independently by a total of three observers experienced in MRCA. The MRCA image sets were analyzed by paging through the source MRCA slice images. First, the number of breath holds and scan duration for each patient was measured. Second, the coverage of coronary anatomy was assessed based on the number of the coronary segments seen in each coronary artery by MRCA compared to X-ray coronary angiography. The coronary segments were identified according to the American Heart Association classification system

(Alderman et al., 1993; Austen et al., 1975). Side branches were not included. Third, image quality of each coronary segment was judged using a semi quantitative grading scale based on the extent of the contiguity of the vessel border of a coronary segment (measured in percentage) and the amount of artifact present in the segment (interruption of the vessel border definition) (Yang et al., 2003b). The scale ranged from 1–4 (1=excellent quality, >91% contiguity of the vessel border of a given segment with minimum artifact; 2=good quality, 75–90% contiguity with minimum to mild artifact; 3=fair quality, 51–74% contiguity with minimum to moderate artifact; and 4=nondiagnostic quality, <50% contiguity). Finally, three observers who were blinded from the findings on the coronary angiogram reviewed the images of the four major coronary arteries to identify CAD. A coronary lesion was defined as a stenosis >50% and was identified by the degree of signal loss compared to an adjacent normal segment. This signal loss may be either smooth or irregular, and symmetric or asymmetric in appearance (Manning et al., 1993; Pennell et al., 1996). Any disagreement in the presence or absence of a coronary lesion among the observers was resolved by consensus.

Coronary Angiography

In all patients, coronary angiography was performed by the transfemoral Judkins approach. Angiograms documented in digitized format allowed spatial resolution of 0.3 mm. Classification of the coronary segments was described above. The X-ray angiography was analyzed by the interventional cardiologists who performed the procedure. The interventional cardiologists were instructed to study the angiographic images directly and to define all stenoses greater than 50% to constitute CAD.

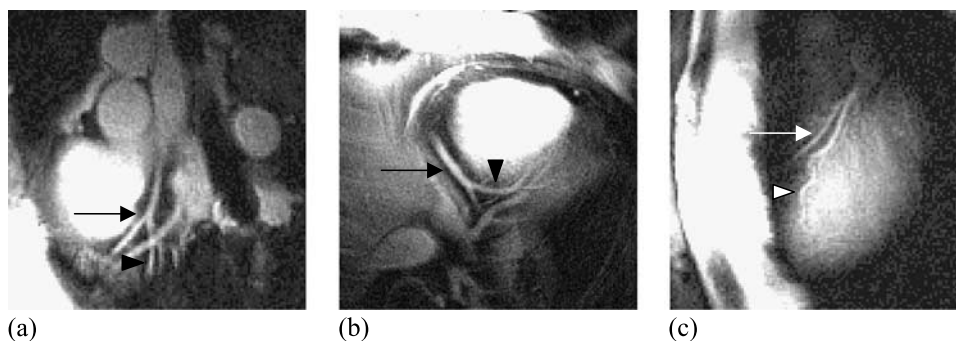


Figure 4. Representative high resolution image of (a) mid-LAD (arrow) and diagonal artery (arrowhead), (b) distal-RCA (arrow) and posterior descending artery (arrowhead), and (c) distal-LAD (arrow) and diagonal artery (arrowhead).

Table 2. Total number (%) of coronary segments seen by *dRT*.

	RCA	LM	LAD	LCx
Proximal	45/45 (100%)	44/44* (100%)	41/41* (100%)	44/44* (100%)
Middle	44/44* (100%)	NA	40/41* (98%)	NA
Distal	38/45 (84%)	NA	34/45 (76%)	26/45 (58%)
Total	127/134 (95%)	44/44 (100%)	115/127 (95%)	70/89 (79%)

Abbreviations: *dRT*=dynamic real-time architecture; NA=not applicable; RCA=right coronary artery; LM=left main artery; LAD=left anterior descending artery; LCx=left circumflex artery.

*Excluded coronary segments due to stent or total occlusion.

Statistical Analysis

The visualization of coronary segments and the detection of diseased and normal coronary arteries were given in percent, specificity, and sensitivity values. The image quality for the coronary segments was given in mean grade value \pm SD. Kappa value was calculated to assess interobserver agreement. A *p*-value less than 0.05 was considered significant.

RESULTS

Scan Time and Breath-Hold Duration

The scan time ranged from 20–45 min with a mean duration and standard deviation of 30 ± 10 minutes. The acquisition time for each coronary scan was less than 16 sec (16 heartbeat breath-hold time). The number of breath holds per patient ranged from 6–23 with mean and standard deviation of 12 ± 8 . All patients tolerated the 16 heartbeat breath hold.

Coverage of Coronary Anatomy

Coronary angiography revealed a total of 394 coronary segments in 45 patients. Eleven segments with stent placement were excluded. The stents created a distinct signal loss at the area of placement. The HR imaged 91% (357/394) of the major epicardial coronary segments seen with coronary angiography. The mean percentage of the coronary segments seen in each coronary artery was: 1) RCA 95% (127/134), 2) LM 100% (44/44), 3) LAD 91% (115/127), and 4) LCx 79% (70/89). Table 1 details the number and percentage of each coronary segment seen in the coronary arteries.

Image Quality of the Coronary Segments

Excellent or good (grade 1–2) image quality was obtained in 86% of all the coronary segments as shown

in Figs. 3 and 4. Fair image quality (grade 3) was obtained in 5% of all coronary segments. Nondiagnostic (grade 4) image quality was demonstrated in approximately 9% of the coronary segments. Table 2 details the mean image quality in each coronary segment.

Detection of the Coronary Stenoses

A total of 40 coronary stenoses were identified on the coronary angiography. There were 2 LM, 13 RCA, 16 LAD, and 9 LCx lesions. Analysis of the coronary arteries by MRCA images yielded an overall sensitivity and specificity of 92% and 88%, respectively, on a per vessel basis in detecting coronary arteries with stenosis. One vessel (LM) was excluded from analysis due to stent placement. On a per patient basis, the sensitivity and specificity were 100% and 77%, respectively, in detecting patients with CAD. Interobserver agreement (kappa) was 0.84 ($p < 0.05$). The frequency of CAD in the population was 51% (23/45). Additional sensitivity and specificity data on the individual RCA, LM, LAD, and LCx arteries are detailed in Table 3. Representative MR and corresponding conventional angiogram images of varying degrees of coronary stenoses are demonstrated in Fig. 5.

Table 3. Sensitivity and specificity (total number) of *dRT* images in the detection of lesions in individual coronary artery and patients with coronary artery disease.

	Sensitivity	Specificity
RCA	100% (13/13)	84% (27/32)
LM	100% (2/2)	93% (39/42)
LAD	94% (15/16)	83% (24/29)
LCx	78% (7/9)	89% (32/36)
Overall (artery)	93% (37/40)	88% (122/139)
Overall (patient)	100% (23/23)	77% (17/22)

Abbreviations: *dRT*=dynamic real-time architecture; RCA=right coronary artery; LM=left main artery; LAD=left anterior descending artery; LCx=left circumflex artery.

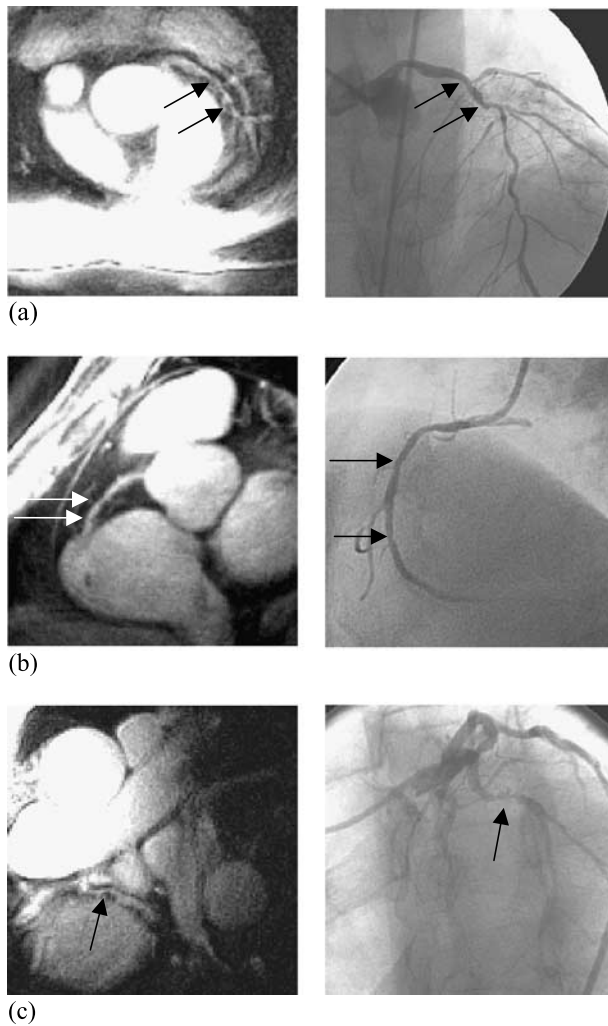


Figure 5. The HR and corresponding angiogram images of varying severity of coronary stenosis (a) 40% distal-LM and 70% proximal-LAD lesions, (b) 40% mid-RCA lesions, and (c) 85% proximal-LCx lesion.

DISCUSSION

The real-time imaging system represents one of the most significant advances in the software development of cardiovascular applications in MR. The first RT acquisition method for multiplanar or echo-planar imaging was developed using NMR spin echoes (Mansfield, 1977). Recent developments have demonstrated an acquisition of a complete image within a period as short as 40 ms yielding a frame rate of 25 complete images/second (Nayak and Hu, 2003). Real-time image reconstruction is also essential. Using a sliding window reconstruction, real-time image display on conventional scanners using FLASH or GRASS sequences was made possible (Riederer et al., 1988).

However, it was not until the development of a robust and reliable RT system in a conventional scanner when routine clinical studies became possible. This RT system enabled ultrafast image acquisition, eliminating the need for cardiac or respiratory gating; interactive selection of the scan plane allowing immediate control of the desired view plane; and real-time image reconstruction and display providing instantaneous image-based feedback (Kerr et al., 1997). A clinical trial to assess cardiac function using this RT system demonstrated reliable imaging of global and regional wall motion (Yang et al., 1998). However, the standard RT architecture only performed continuous acquisition of an identical pulse configuration. No integration of different sequences was possible in real time. Only limited modifications including scaling of preexisting waveform and alterations of simple timing parameters were possible. The *dRT* addressed these limitations by integrating multiple sequences through dynamic reconfiguration of pulse sequences.

In this study, we validated the *dRT* in MRCA through a prospective clinical trial of patients suspected of coronary artery disease. Although recent clinical trials had demonstrated encouraging results, MRCA continues to play a limited clinical role (Kim et al., 2001; Manning et al., 1993). In order to become more than just a research tool, MRCA must simplify its scan protocols, improve image quality, and increase anatomic coverage. The *dRT* represented an optimal framework for MRCA, allowing dynamic utilization of multiple sequences and coil elements. The integration of real-time and high-resolution imaging sequences allowed excellent image quality, anatomic coverage, and detection of coronary stenosis. Per acquisition adjustments enabled precise RT localization of the coronary plane followed by immediate HR-based feedback, allowing rapid improvement of the image quality or characterization of a coronary lesion. This adaptive architecture also allowed evaluation of the displacement of the coronary artery due to a patient's breath hold prior to the acquisition of high-resolution image. Thus, the imaging plane was adjusted rapidly in RT to compensate for the breath-hold position. Incorporated into the adaptive real-time system was a customized coronary coil designed to improve SNR and anatomic coverage. The coil consisted of two coil elements to target the proximal, mid- and distal sections of the four major coronary arteries. The *dRT* architecture enabling the real-time switch between the two elements facilitated acquisition of high-quality images.

Another key feature of the *dRT* system was the implementation of spiral imaging. Although spiral acquisition is known for its sensitivity to off-resonance

spins and field inhomogeneity, comparative studies have reported improved imaging efficiency of spiral technique over the commonly used segmented k-space approaches in MRCA (Bornert et al., 2001; Keegan et al., 1999; Meyer et al., 1992; Taylor et al., 2000). High temporal resolution, achieved through efficient data collection and rapid k-space coverage, resulted in short acquisition time. This minimizes the blurring often seen in the segmented k-space strategy (Hofman et al., 1996, 1998; Wang et al., 1999). Improved spatial resolution was obtained through full k-space coverage instead of partial k-space coverage in segmented approach (Meyer et al., 1992). Image artifacts were reduced through excellent flow characteristics of spirals due to small phase shifts in the k-space origin (Nishimura et al., 1995). The ability to require only a single excitation per heartbeat per slice allowed larger flip-angle excitation generating higher SNR (Meyer et al., 1992). Finally, CNR was enhanced by more robust fat suppression through spectral-spatial excitation rather than conventional fat saturation (Meyer et al., 1990).

In comparison to the prior clinical trial utilizing real-time coronary localization, the *dRT* represents a fundamental change in RT imaging paradigm (Yang et al., 2003a). Although different patients were enrolled not allowing any direct comparison, this architecture enabled a complete coronary exam with fewer number of breath holds and shorter scan time. A higher percentage of coronary segments were visualized with excellent to good image quality, resulting in a more accurate detection of diseased coronary arteries.

Limitations

The *dRT* represents an optimal imaging platform for routine clinical implementation of MRCA. Other important features, however, must be integrated into the system. First, additional contrast to enhance the visualization of the distal LAD and LCx segments by suppressing the surrounding structures is necessary. While fat is well suppressed, strategies to improve the contrast-to-noise ratio by suppressing the competing signals from the surrounding myocardium would be desirable. Contrast mechanisms including magnetization transfer, T2-prep, steady-state free precession, and inversion prepulse with intravascular contrast agent must be incorporated into the architecture so that rapid and flexible selection of the desired contrast technique is possible (Brittain et al., 1995; Hu et al., 1992; Lorenz and Johansson, 1999; Vasanawala et al., 1999). Second, improvement in the coverage of tortuous coronary anatomy must be made. Reliable imaging of

tortuous vessels extending into multiple planes will be possible by three-dimensional (3D) imaging using the stack of spirals technique (Thedens et al., 1999). While inherent difficulties exist in 3D spiral techniques, some trade-offs may become necessary for robust imaging of anatomical variations. Third, improved coil designs, such as a three-element triangular phased array or an additional posterior element, may address the image quality of distal coronary segments along the lateral and posterior walls (Fayad et al., 1995). The current coil design is limited by the smaller 4-in. elements. While higher sensitivity volume and SNR are achieved than standard five-in. surface coil or phased-array cardiac coil, reduced penetration into the posterior regions may explain the image quality achieved in distal LCx and LAD (Engvall et al., 2003). Fourth, shorter breath-hold duration is always desirable. While all patients tolerated the breath holds in this study, shorter breath holds may be achieved by faster image acquisition techniques employing the variable density spiral technique (Lee et al., 2001). Alternatively, navigator-based nonbreathing approaches such as the diminished variance algorithm in free-breathing 3D spiral MRCA sequence needs to be investigated (Sachs et al., 2000; Thedens et al., 1999). In addition, the sensitivity and specificity data for the detection of CAD could be improved by better characterization of the signal loss from the calcium in the plaque. A short-axis view of the stenosis may differentiate calcium in the vessel wall and better delineate the luminal extent of the plaque. Finally, patient recruitment may have been problematic. The pretest probability of the subjects was high as they were patients referred for cardiac catheterization. A cohort with lower prevalence of CAD would reduce such bias.

CONCLUSION

In conclusion, our study validates the use of *dRT* in MRCA. This prospective clinical trial provides data supporting a potential clinical role of this rapid, flexible, and robust imaging architecture. Efforts to implement *dRT* architecture in conventional scanners will facilitate noninvasive imaging of coronary artery disease.

ACKNOWLEDGMENTS

This study was supported by grants 5K23 HL04338-02 and HL39297 from the National Heart,

Lung, and Blood Institute of NIH, General Electric Medical Systems, and Donald W. Reynolds Foundation. Financial support: National Heart, Lung, and Blood Institute, NIH, Bethesda, MD; General Electric Medical Systems, Milwaukee, MI; Donald W. Reynolds Foundation, Las Vegas, NV.

REFERENCES

- Alderman, E., Corley, S., Fisher, L., et al. (1993). Five-year angiographic follow-up of factors associated with progression of coronary artery disease in the Coronary Artery Surgery Study (CASS). *J. Am. Coll. Cardiol.* 22:1141–1154.
- Austen, W., Edwards, J., Frye, R., et al. (1975). A reporting system on patients evaluated for coronary artery disease. In: *Report of the Ad Hoc Committee for Grading Coronary Artery Disease, Council on Cardiovascular Surgery*. Vol. 51. American Heart Association. 5–40.
- Bornert, P., Stuber, M., Botnar, R., Kissinger, K.V., Koken, P., Spuentrup, E., Manning, W.J. (2001). Direct comparison of 3D spiral vs. cartesian gradient-echo coronary magnetic resonance angiography. *Magn. Reson. Med.* 46:789–794.
- Brittain, J., Hu, B., Wright, G., Meyer, C., Macovski, A., Nishimura, D. (1995). Coronary angiography with magnetization prepared T2 contrast. *Magn. Reson. Med.* 33:689–696.
- Engvall, J., Scott, G., Santos, J., Nguyen, P., Amitai, M., McConnell, M., Pauly, J., Nishimura, D., Hu, B., Yang, P. (2003). MR coronary angiography using a novel 2-element phased-array coil: improved image quality and anatomic coverage [Abstract]. *J. Cardiovasc. Magn. Reson.* 5:290–291.
- Fayad, Z., Connick, T., Axel, L. (1995). An improved quadrature or phased-array coil for MR cardiac imaging. *Magn. Reson. Med.* 34:186–193.
- Hofman, M., van Rossum, A., Sprenger, M., Westerhof, N. (1996). Assessment of flow in the right human coronary artery by magnetic resonance phase contrast velocity measurement: effects of cardiac and respiratory motion. *Magn. Reson. Med.* 35:521–531.
- Hofman, M., Wickline, S., Lorenz, C. (1998). Quantification of in-plane motion of the coronary arteries during the cardiac cycle: implications for acquisition window duration for MR flow quantification. *J. Magn. Reson. Imaging* 8:568–576.
- Hu, B., Conolly, S., Wright, G., Nishimura, D., Macovski, A. (1992). Pulsed saturation transfer contrast. *Magn. Reson. Med.* 33:689–696.
- Keegan, J., Gatehouse, P., Taylor, A., Yang, G., Jhooti, P., Firmin, D. (1999). Coronary artery imaging in 0.5-tesla scanner: implementation of real-time, navigator echo-controlled segmented k-space FLASH and interleaved spiral sequences. *Magn. Reson. Med.* 41:392–399.
- Kerr, A., Pauly, J., Hu, B., Li, K.C., Hardy, C.J., Meyer, C.H., Macovski, A., Nishimura, D.G. (1997). Real-time interactive MRI on a conventional scanner. *Magn. Reson. Med.* 38:355–367.
- Kim, W., Danias, P., Stuber, M., Flamm, S.D., Plein, S., Nagel, E., Langerak, S.E., Weber, O.M., Pedersen, E.M., Schmidt, M., Botnar, R.M., Manning, W.J. (2001). Coronary magnetic resonance angiography for the detection of coronary stenoses. *N. Engl. J. Med.* 345:1863–1869.
- Lee, J., Hargreaves, B., Nishimura, D. (2001). Fast 3D imaging using variable density spiral trajectories [Abstract]. In: *Proc. ISMRM 9th Annual Meeting*. 1777.
- Li, D., Carr, J., Shea, S., Zheng, J., Deshapande, V.S., Wielopolski, P.A., Finn, J.P. (2001). Coronary arteries: magnetization-prepared contrast-enhanced three-dimensional volume-targeted breath-hold MR angiography. *Radiology* 219:270–277.
- Lorenz, C., Johansson, L. (1999). Contrast-enhanced coronary MRA. *J. Magn. Reson. Imaging* 10:703–708.
- Manning, W., Li, W., Edelman, R. (1993). A preliminary report comparing magnetic resonance coronary angiography with conventional angiography. *N. Engl. J. Med.* 328:828–832.
- Mansfield, P. (1977). Multi-planar image formation using NMR spin echos. *J. Phys. C: Solid State Phys.* 10:L55–L58.
- Meyer, C., Pauly, J., Macovski, A., Nishimura, D. (1990). Simultaneous spatial and spectral selective excitation. *Magn. Reson. Med.* 35:521–531.
- Meyer, C., Hu, B., Nishimura, D., Macovski, A. (1992). Fast spiral coronary artery imaging. *Magn. Reson. Med.* 28:202–213.
- Nayak, K., Hu, B. (2003). Triggered real-time MRI and cardiac applications. *Magn. Reson. Med.* 49:188–192.
- Nishimura, D., Irarrazabal, P., Meyer, C. (1995). A velocity k-space analysis of flow effects in echo-planar and spiral imaging. *Magn. Reson. Med.* 33:549–556.
- Pennell, D., Bogren, H., Keegan, J., Firmin, K., Underwood, S. (1996). Assessment of coronary artery stenosis by magnetic resonance imaging. *Heart* 75:127–133.
- Riederer, S., Tasciyan, T., Farzaneh, F., Lee, J., Wright,

- R., Herfkens, R. (1988). MR fluoroscopy: technical feasibility. *Magn. Reson. Med.* 8:1–15.
- Sachs, T., Meyer, C., Pauly, J., Hu, B., Nishimura, D., Macovski, A. (2000). Real-time interactive 3D-DVA for robust coronary MRA. *IEEE Trans. Med. Imag.* 19:73–79.
- Santos, J., Wright, G., Yang, P., Pauly, J. (2002). Adaptive Architecture for real-time imaging systems [Abstract]. In: Proc. ISMRM 10th Annual Meeting. 468.
- Taylor, A., Keegan, J., Jhooti, P., Gatehouse, P., Firmin, D., Pennell, D. (2000). A comparison between segmented k-space FLASH and interleaved spiral MR coronary angiography sequences. *J. Magn. Reson. Imaging* 11:394–400.
- Thedens, D., Irarrazabal, P., Sachs, T., Meyer, C., Nishimura, D. (1999). Fast magnetic resonance coronary angiography with a three-dimensional stack of spiral trajectory. *Magn. Reson. Med.* 41:1170–1179.
- Vasanawala, S., Pauly, J., Nishimura, D. (1999). Fluoroscopic equilibrium MRI. *Magn. Reson. Med.* 42:876–883.
- Wang, Y., Vidan, E., Bergman, G. (1999). Cardiac motion of coronary arteries: variability in the rest period and implications for coronary MR angiography. *Radiology* 213:751–758.
- Yang, P., Kerr, A., Liu, A., Meyer, C.H., Macovski, A., Pauly, J.M., Hu, B.S. (1998). New real-time interactive cardiac magnetic resonance imaging system complements echocardiography. *J. Am. Coll. Cardiol.* 32:2049–2056.
- Yang, P., Meyer, C., Kerr, A., Terashima, M., McConnell, M., Kaji, S., Macovski, A., Pauly, J., Nishimura, D., Hu, B. (2003). Spiral magnetic resonance coronary angiography with real-time localization. *J. Am. Coll. Cardiol.* 41:1134–1141.
- Yang, P., Nguyen, P., Shimakawa, A., Brittain, J., McConnell, M., Hu, B., Spiral, M. R. (2003). Coronary angiography with real-time localization at 3T[Abstract]. *J. Am. Coll. Cardiol.* 41:432A.

Submitted February 12, 2004

Accepted June 10, 2004